PHYSICAL REVIEW B VOLUME 18, NUMBER 6 15 SEPTEMBER 1978

Optical properties of expanded fluid mercury

H. Ikezi, K. Schwarzenegger, A. L. Simons, A. L. Passner, and S. L. McCall
Bell Laboratories, Murray Hill, New Jersey 07974

(Received 16 September 1977)

The optical-reflectivity measurements of expanded fluid mercury indicate a significant decrease of the optical conductivity which appears at the low frequencies when the metal–nonmetal transition occurs. The relation of the localization of electronic states is discussed.

I. INTRODUCTION

A simple band model predicts that divalent metals are transformed to an insulating state if the density of atoms is reduced sufficiently. Since liquid Hg has relatively low critical temperature and pressure (about 1500 °C and 1.5 kbar), it can be expanded continuously from liquid to gaseous densities. The measurements of the electrical conductivity,[1–4] the Hall coefficient,[4] and the thermoelectric power[2,3] of fluid Hg indicate that a gradual transition from metallic to semiconducting states occurs at a density of about 9 $\mathrm{g/cm^3}$ (roughly 65% of normal liquid-Hg density at room temperature) upon its expansion. On the other hand, an extrapolation of the optical-absorption experiments[5,6] has shown that an optical band gap appears when the density ρ is below about 5.5 $\mathrm{g/cm^3}$, which does not agree with the density where the metal-nonmetal transition takes place.

It has been thought that a depression in the electronic density of states or a "pseudogap" causes the metal-semiconductor transition and evolves into the atomic $6s$ and $6p$ states.[7] Two conflicting models for the transition of electronic transport have been proposed; one is based on localization of electronic states induced by disorder[8] and the other considers inhomogeneities due to fluctuations.[9] The results of Knight-shift measurements[10] are inconsistent with either of these theories. In short, the mechanisms of electronic transport near the transition in fluid Hg is a controversial subject.

Since mercury becomes opaque when the density is higher than 4.5 $\mathrm{g/cm^3}$, the optical-absorption measurements are difficult in the crucial density region where metal-nonmetal transition occurs.[6] In this paper, we report the first optical-reflectivity measurements for expanded fluid Hg. The measurements, in a frequency range $0.3\ \mathrm{eV} \leq \hbar\omega \leq 3\ \mathrm{eV}$, are extended from the normal liquid-metal density to the density where the absorption-gap appears. Our data provide the information on the electronic density of states.

II. EXPERIMENTAL APPARATUS

Both reflection and absorption were measured by use of an internally heated autoclave. The sample cell mounted in the autoclave consisted of a molybdenum cylinder (degassed in a hydrogen oven), closed at both ends with synthetic sapphire windows. A narrow gap between the sapphire window surfaces was filled with triple-distilled mercury under vacuum to avoid trapped or dissolved gases. Argon gas was used as a medium to control pressure. A W-WRe thermocouple for the measurements of sample temperature was calibrated by employing vapor-pressure curve obtained by Hensel.[11] The vaporization temperature at a given pressure can be easily found because the sample becomes transparent when it is vaporized. Values of the density for each set of the temperature T and the pressure p were determined from the data compiled by Schmutzler.[12] Although we can measure the temperature within an error of ±10 °C, the densities obtained from compilation and extrapolation of experimental data in Ref. 12 have large uncertainties, especially in a region $5 < \rho < 8\ \mathrm{g/cm^{-3}}$. Among others, this uncertainty introduces the largest error in our data. We therefore show the pressure and the temperature for each experimental curve in addition to the density.

A standard optical setup was employed to measure the reflectivity. The optical system consisted of a high-pressure xenon lamp, a KBr prism monochrometer, the aluminum-coated mirrors, and the indium antimonide and silicon detectors. The reflectivity data to be presented here is for the incident light nearly normal (about 2° off from normal incidence) to a surface between Hg and optically polished sapphire. The optical path in the sapphire window makes an angle of 60° with respect to the c axis of the window. The entire optical system was calibrated by use of reflection at the sapphire-vacuum interface.[13] A small error due to temperature-dependent absorption in sapphire is corrected by the use of data of absorption.[14]

© 1978 The American Physical Society

In the absorption experiments, we measured the attenuation of the light intensity in the sample of the thickness of 50 and 100 μm.

III. ANALYSIS OF REFLECTIVITY

The results of reflectivity measurements are plotted by solid lines in Fig. 1. Typical metallic reflectivity curves are obtained when the density is higher than 12 g/cm^3. Namely, the enhanced reflectivity is observed in the low-frequency range. The reflectivity decreases at smaller densities, and less enhancement of R at low frequencies is found. When $\rho \lesssim 9$ g/cm^3, the reflectivity curves show semiconductor-like behavior; the value of R has a maximum between 1 and 2 eV and falls off at both high and low frequencies.

In order to discuss the structure of the electronic density of states, we are interested in the conductivity σ as a function of the frequency ω. Many authors[15] have obtained the optical conductivity from the reflectivity by employing the Kramers-Kronig relation. However, this method is not applicable in our case because the sapphire, which is transparent in a limited frequency range, is the only window material available which works at high temperature. The ellipsometric measurements[16] are also not useful because the sapphire is anisotropic.

To find the conductivity, we consider the following properties of the reflectivity. (i) The Drude model accounts for the optical properties of normal liquid Hg.[15,16] In fact, we have observed typical metallic reflectivity when $\rho \gtrsim 12$ g/cm^3. (ii) At lower densities, the reflectivity curves show semiconductorlike behavior, indicating that $\sigma(\omega=0)$ vanishes. Since $\int \sigma_r(\omega)d\omega$ ($\sigma_r = \mathrm{Re}\sigma$) has to be finite, σ_r must have peak(s) at finite ω. A model dielectric function

$$\begin{aligned}\epsilon(\omega) &= \epsilon_r + i\epsilon_i \\ &= 1 - \frac{\omega_{p0}^2}{\omega(\omega+i\nu_0)} - \sum_{l=1} \frac{\omega_{pl}^2}{\omega(\omega+i\nu_l)-\omega_l^2}\,, \qquad (1)\end{aligned}$$

satisfies above requirements. We expect that the first two terms on the right-hand side of Eq. (1) account for the observed reflectivity when the density is high. The last resonance terms are thought to be important when the density is decreased. The expression (1) is consistent with the theory based on the localization[8] predicting σ_r is proportional to ω^2 when ω is small.

By using the relations

$$R = \frac{(n_r - n_0)^2 + n_i^2}{(n_r + n_0)^2 + n_i^2}\,, \quad \tilde{n} \equiv n_r + i n_i = \epsilon^{1/2}, \qquad (2)$$

$$\mathrm{Re}\sigma \equiv \sigma_r = \omega\epsilon_i / 4\pi\,,$$

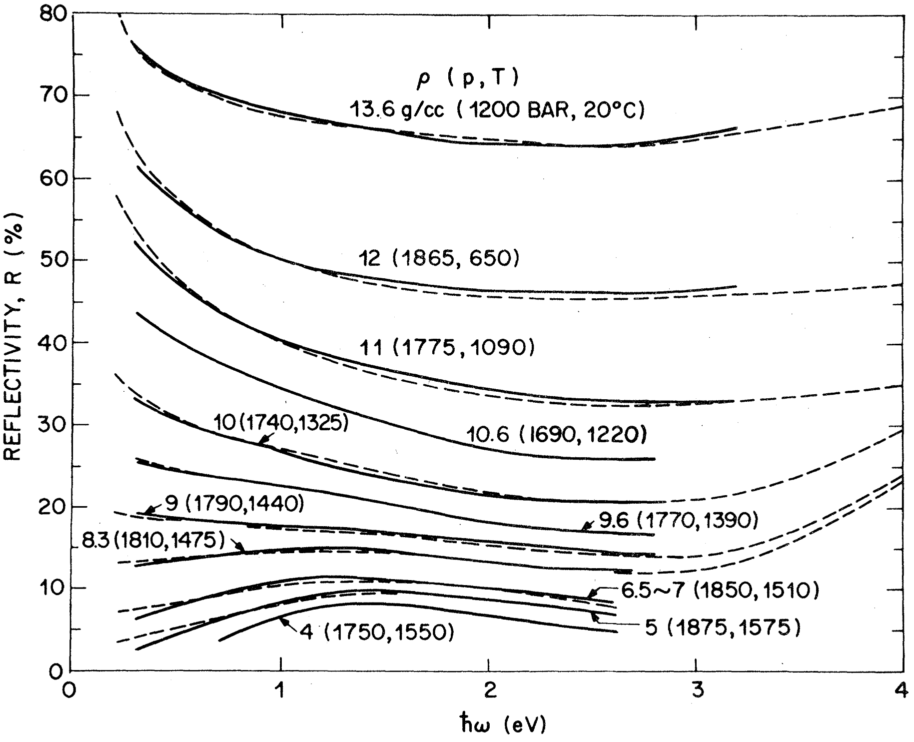

FIG. 1. Reflectivity as a function of frequency at different densities. Solid lines; experimental values. Dashed lines; calculated values by using Eqs. (1)–(3). The numbers labeled on each line are the density in g/cm^{-3}, the pressure in bar, and the temperature in °C.

and sum rule

$$\int \sigma_r \, d\omega = \frac{1}{4} \sum_{l=0} \omega_{pl}^2 = \frac{\pi n e^2}{m} , \qquad (3)$$

we look for the parameters ω_{pl}^2, ω_l^2, and ν_l in such a way that the calculated reflectivities R fit the experimental curves. Here, n_0 is the index of refraction of sapphire.[13] We assume two electrons per atom to find the electron density n and use the mass of free electrons m. Although one may employ a series expansion of σ_r in ω for instance, we chose the form of Eq. (1), because Eq. (1) yields a simple form of the sum rule (3) so that the numerical processing is simpler.

We give the initial values of parameters and start the trial and error fitting process. If the initial values are not too much different from the realistic values, the computer finds a good set of final values. We have changed the number of resonance terms in Eq. (1) to check the error arising from the use of finite number of terms. We have obtained fairly good fitting by using two broad-resonance terms. The fitting is slightly improved if three resonance terms are used. We have found that Eq. (1) is not appropriate to describe observed R when $\rho < 5$ g/cm^3.

IV. RESULTS AND DISCUSSIONS

The real part of the conductivity $\sigma_r(\omega)$ plotted in Fig. 2 is obtained by employing the fitting process described in Sec. III. The calculated reflectivities corresponding to each conductivity curve are shown in Fig. 1 by dashed lines. When $\rho \gtrsim 12$ g/cm^3, the reflectivities calculated only from the first two terms on the right-hand side of Eq. (1) (Drude model) fit the observed reflectivities, indicating that the nearly-free-electron model adequately describes the conductivity.[15] The theorem of Edwards[17] shows that the density of state of electrons does not appear in the conductivity expression works in this high-density regime. At densities below 11 g/cm^3, the terms at least up to $l = 2$ in Eq. (1) are necessary in order to account for observed reflectivity. This change in the characteristic of dielectric function would coincide with the appearance of a "pseudogap" or diffusive conduction regime.[4,18] The dc conductivity, $\sigma_r(0) = \omega_{p0}^2 / 4\pi\nu_0$ estimated from our reflectivity measurements agrees fairly well with the results of dc conductivity measurements by Schmutzler and Hensel[2] (shown by arrows in Fig. 2).

Small reflectivities, $R < 0.2$, are observed at the

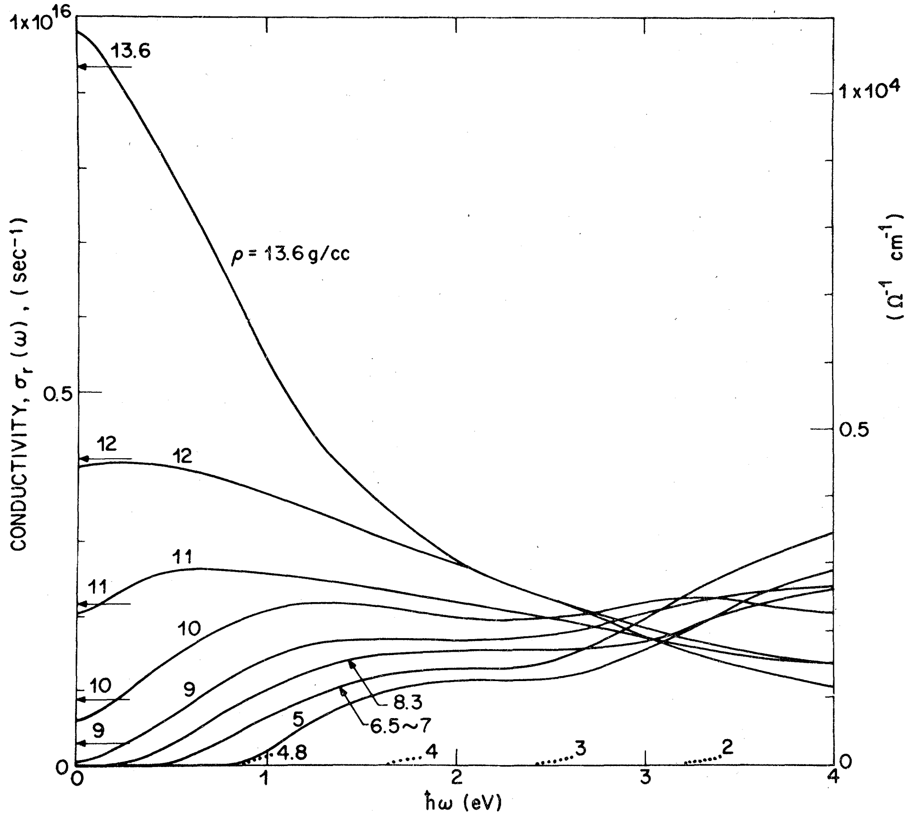

FIG. 2. Calculated conductivity by using observed reflectivity data ($\rho \geq 5$ g/cm^{-3}) and absorption data ($\rho \leq 4.8$ g/cm^{-3}) by Uchtman and Hensel, Ref. 6. We have used $\sigma_r = (c\epsilon_r^{1/2}/2\pi)K$ and $\epsilon_r^{1/2} = 3$.

densities around 8 g/cm^3 where the characteristics of dc conductivity and thermoelectric power indicate that a gradual transition from the metallic to the semiconducting states occurs. As we see in Fig. 2, this small reflectivity results in a small $\sigma_r(\omega)$; the contribution to the integral $\int \sigma_r \, d\omega$ from the range of measurements, $\hbar\omega < 3$ eV, is much smaller than $\pi n e^2/m$. The sum rule (3), therefore, indicates that $\sigma_r(\omega)$ must be large in the frequency range, $\hbar\omega > 3$ eV. We therefore need conductivity peak appearing above 3 eV. Although the sum rule specifies only the cross section under this peak, the peak position is not arbitrary because σ_i, corresponding to the peak of σ_r, changes the real part of ϵ so that it changes the reflectivity in the low-frequency region. Our fitting process has also found that ω_{p0}^2 vanishes when $\rho < 8$ g/cm^3.

In order to consider the electronic density of states $N(E)$, we employ an expression for the conductivity[19]

$$\sigma(\omega) = \frac{2\pi e^2 \hbar^2 \Omega}{m^2 \omega} \int_{E_F - \hbar\omega}^{E_F} N(E) N(E + \hbar\omega) |D|^2 \, dE \,, \qquad (4)$$

where D is the matrix element of $\partial/\partial x$, Ω is the volume, and the other notations are standard ones. If $|D|^2$ does not change rapidly, then σ_r is given as the convolution of N. The conductivity curves in Fig. 2 have a double-step shape as depicted in Fig. 3(a) when $\rho < 8$ g/cm^3. The conductivity expression (4) indicates two possible profiles of $N(E)$ as shown in Figs. 3(b) and 3(c). At this low-density regime, the density of states has a depression of the width of $\hbar\omega_d$ which is larger than 3 eV. A shoulder of σ_r appearing between 1 and 2 eV indicates the existence of hump in the depression of $N(E)$.

The optical absorption measurements in a low-density regime, $\rho \leq 4.8$ g/cm^3 by Uchtman and Hensel[6] and by ourselves (shown in Fig. 4) reveal an exponential change of the extinction coefficient $K(\omega)$. $K(\omega)$ increases an order of magnitude when $\hbar\omega$ changes a few tenths of eV.

We employ a relation

$$\sigma_r = (cK/2\pi)[(cK/\omega)^2 + \epsilon_r]^{1/2} \,, \qquad (5)$$

to obtain σ_r from the absorption measurements. From the observed reflectivity $R < 0.1$ for $\rho < 5$ g/cm^3 and Eq. (2), we find $1 \lesssim \epsilon_r^{1/2} \lesssim 3$. In the parameter range of the absorption measurements, $(cK/\omega)^2$ is much smaller than ϵ_r. We find that the highest observed value of K in Ref. 6, 1×10^4 cm^{-1}, gives rise to $\sigma_r = (0.3-1) \times 10^{14}$ sec^{-1} (=30–100 Ω^{-1} cm^{-1}). Therefore, the absorption measurements see only a part of small conductivity tail as shown in Fig. 2 by dotted lines. The conductivity curves deduced from the reflectivity are fairly consistent with σ_r estimated from $K(\omega)$ given in Ref. 6 at $\rho \simeq 5$ g/cm^3.

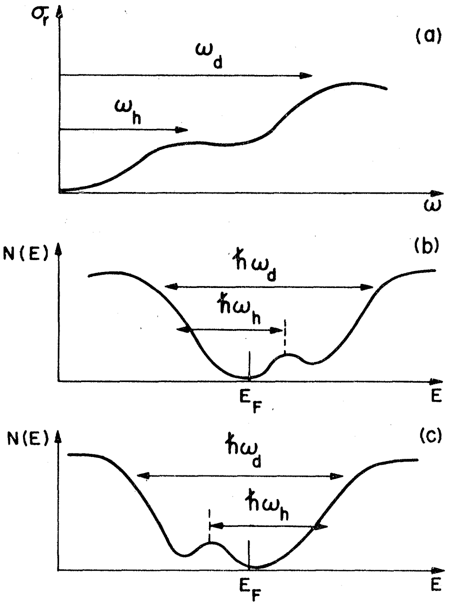

FIG. 3. Schematic curves of σ_r and $N(E)$.

By using Eq. (4), the absorption measurements enable us to discuss the structure of $N(E)$. The observed K as a function of ω indicates that the bottom of the conduction band and the top of the valence band are well separated in the low-density regime where the absorption measurements can be performed. As we have shown, the absorption measurements observe a part of small conductivity tail so that it observes a part of small $N(E)$.

According to the arguments described in Ref. 7, the electronic states are localized when $g(E)$ [$\equiv N(E)/N_{\text{fe}}(E)$] is smaller than about 0.3. Here $N_{\text{fe}}(E)$ is a free-electron value. The localization effect introduces the mobility edges E_c and E_v defined by $g(E_{c,v}) \sim 0.3$ at the bottom of the conduction and the top of the valence bands. When the mobility gap given by $E_c - E_v$ vanishes, the transition to the metallic state occurs. The minimum dc conductivity σ_0 at the transition is found to be about 300 Ω^{-1} cm^{-1}. In order to find the gap width from the optical data, we employ an expression for the conductivity when $\hbar\omega = \hbar\omega_g \equiv E_c - E_v$,

$$\sigma(\omega_g) = \sigma_0 4\Delta E/\hbar\omega_g, \quad \text{for } 4\Delta E < \hbar\omega_g, \qquad (6)$$

where ΔE is the width of the localized states [see Fig. 2 and Eq. (8) in Ref. 19]. If we choose that ΔE equals e-folding energy of K which is about 0.2 eV then we have $\sigma(\omega_g) \simeq 80$ Ω^{-1} cm^{-1} when $\hbar\omega_g = 3$ eV. This is approximately the highest observed

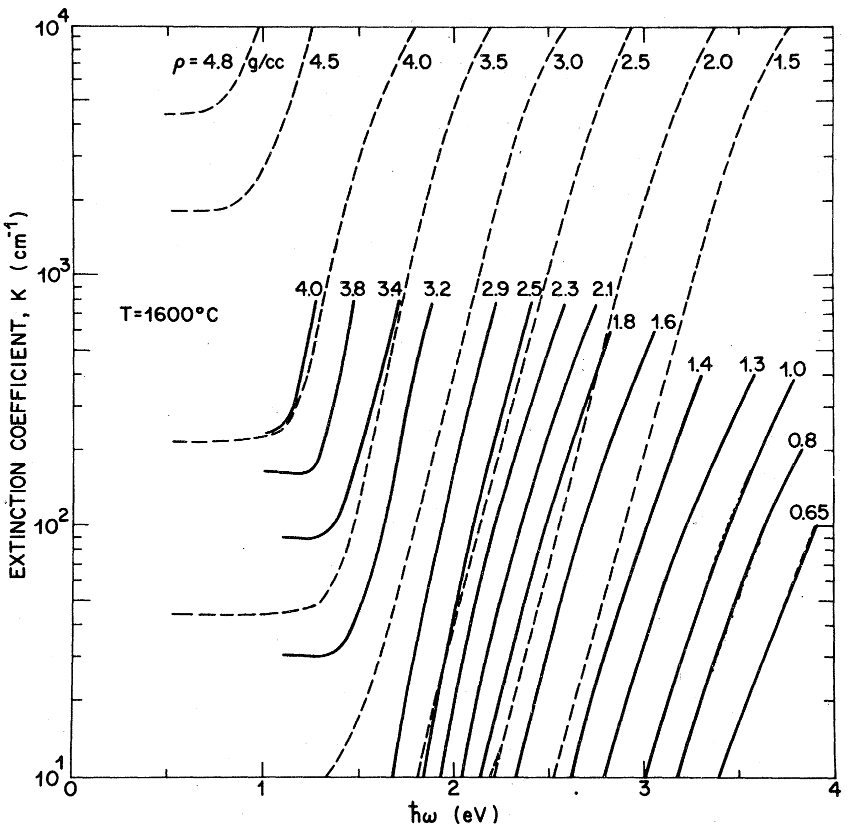

FIG. 4. Extinction coefficient as a function of frequency at different densities. Solid lines; present experiment. Dashed lines; data by Uchtman and Hensel, Ref. 6.

value of $\sigma(\omega)$ in Ref. 6. The conductivity $\sigma(\omega_g)$ is larger when ω_g is smaller. We now find that the absorption measurements have seen the interband transitions of the localized electrons, if we accept the localization theory. Therefore, the width of the mobility gap must be larger than the gap estimated from the absorption data by an *ad hoc* manner.[20] Our reflectivity measurements indicate that such a gap closes at the density of dc conductivity transition.

ACKNOWLEDGMENTS

The authors appreciate advice given by F. Hensel during the development of high-temperature autoclave. We thank R. Bhatt, A. Jayaraman, L. F. Mattheiss, D. B. McWhan, P. M. Platzman, T. M. Rice, M. Schlüter, R. W. Schmutzler, C. M. Surko, M. Uchtman, and W. W. Warren, Jr. for their useful discussions and support, and A. L. Stevens for his technical assistance.

---

[1] E. U. Frank and F. Hensel, Phys. Rev. 141, 109 (1966).

[2] R. W. Schmutzler and F. Hensel, Ber. Bunsenges. Phys. Chem. 76, 531 (1972).

[3] L. J. Duckers and R. G. Ross, Phys. Lett. A 30, 715 (1972).

[4] U. Even and J. Jortner, Phys. Rev. Lett. 28, 31 (1972); Phys. Rev. B 8, 2536 (1973).

[5] F. Hensel, Phys. Lett. A 31, 88 (1970); Ber. Bunsenges. Phys. Chem. 75, 847 (1971).

[6] H. Uchtman and F. Hensel, Phys. Lett. A 53, 239 (1975).

[7] See, for instance, N. F. Mott, *Metal-Insulator Transitions* (Barnes and Nobles, New York, 1974), Chap. 1.

[8] N. F. Mott, Philos. Mag. 22, 7 (1970).

[9] M. H. Cohen and J. Jortner, Phys. Rev. Lett. 30, 699 (1973); Phys. Rev. A 10, 978 (1974).

[10] U. El-Hanany and W. W. Warren, Jr., Phys. Rev. Lett. 34, 1276 (1975).

[11] F. Hensel, dissertation (Universität Karlsruhe, 1966) (unpublished).

[12] R. W. Schmutzler, dissertation (Universität Karlsruhe, 1971) (unpublished). The data are compiled from F. Hensel, Ref. 11; I. Kikoin and A. R. Senchenkov, Fiz. Met. Metalloved. 24, 843 (1967) [Phys. Metals Metallogy. 24, 74 (1967)]; D. R. Posthill, R. G. Ross,

and N. E. Cusack, Philos. Mag. 18, 519 (1968).
[13] I. H. Malitson, F. V. Murphy, Jr., and W. S. Rodney, J. Opt. Soc. Am. 48, 72 (1958).
[14] I. H. Malitson, J. Opt. Soc. Am. 52, 1377 (1962).
[15] E. G. Wilson and S. A. Rice, Phys. Rev. 145, 55 (1966); A. N. Bloch and S. A. Rice, *ibid*. 185, 933 (1969).
[16] J. N. Hodgson, Philos. Mag. 4, 183 (1959).
[17] S. F. Edwards, Philos. Mag. 6, 617 (1962).
[18] L. Friedman, J. Non-Cryst. Solids, 6, 329 (1971).
[19] E. A. Davis and N. F. Mott, Philos. Mag. 22, 903 (1970).
[20] M. A. C. Devillers, J. Phys. F 4, L236 (1974).